

See discussions, stats, and author profiles for this publication at: <http://www.researchgate.net/publication/235259155>

Ion exchange equilibrium and structural changes in clinoptilolite irradiated with β - and γ -radiation. Part II: Divalent cations

ARTICLE *in* EUROPEAN JOURNAL OF MINERALOGY · AUGUST 2008

Impact Factor: 1.48 · DOI: 10.1127/0935-1221/2008/0020-1802

CITATIONS

4

READS

56

3 AUTHORS, INCLUDING:



Daniel Moraetis

Sultan Qaboos University

31 PUBLICATIONS 119 CITATIONS

SEE PROFILE



G.E. Christidis

Technical University of Crete

48 PUBLICATIONS 690 CITATIONS

SEE PROFILE

Ion exchange equilibrium and structural changes in clinoptilolite irradiated with β - and γ -radiation. Part II: divalent cations

DANIEL MORAETIS*, GEORGE E. CHRISTIDIS and VASILIOS PERDIKATIS

Department of Mineral Resources Engineering, Technical University of Crete, 73100, Chania, Greece

*Corresponding author, e-mail: moraetis@mred.tuc.gr

Abstract: Thermodynamic calculations of ion exchange for divalent cations were made for clinoptilolite in natural state and after irradiation with three different doses of β -radiation (10^{12} , 10^{15} and 3×10^{16} e/cm²) and γ -radiation (70 Mrad). The samples were equilibrated with binary systems of divalent cations, namely $\text{Sr}^{2+} \leftrightarrow 2\text{Na}^+$, $\text{Ca}^{2+} \leftrightarrow 2\text{Na}^+$ and $\text{Mg}^{2+} \leftrightarrow 2\text{Na}^+$ at 25 °C and total solution normality of 0.025 N. The selectivity order $\text{Sr}^{2+} > \text{Ca}^{2+} > \text{Mg}^{2+}$ was observed in non-irradiated clinoptilolite. After irradiation with γ -radiation the affinity of clinoptilolite for Sr^{2+} increased and that for Mg^{2+} decreased, whereas the affinity for Ca^{2+} remained unchanged. Irradiation with β -radiation influences selectivity order and clinoptilolite affinity decreases for Sr^{2+} , whereas it increases for Ca^{2+} . For the sample irradiated with maximum dose of β -radiation the selectivity was almost identical for Ca^{2+} and Sr^{2+} . The crystallographic parameters and exchangeable cation site coordinates were refined for all samples with the Rietveld method. The structure refinement of Sr^{2+} -saturated samples yielded changes both in exchangeable sites and site occupancy in channels A and B after irradiation with β - and γ -radiation. The cation sites Sr1 and Sr3 exhibit major changes both in site coordinates and site occupancy after irradiation with β -radiation. In addition, irradiation with γ -radiation yielded major changes in Sr1 occupancy, whereas coordinates changed only slightly. These structural modifications control the observed changes in thermodynamic parameters after irradiation.

Key-words: clinoptilolite, ion exchange, β -radiation, γ -radiation, thermodynamics, Rietveld refinement.

Introduction

The ion exchange of divalent cations in natural clinoptilolite has been examined extensively in the past (Ames, 1964; Loizidou, 1982; Jama & Yucel, 1990; Pabalan, 1994; Pabalan & Bertetti, 1994, 1999). Ion exchange among unequal charge ions is influenced by the concentration-valency effect (Pabalan & Bertetti, 1994). Entropy changes drives ion exchange of unequal charge ions in zeolites owing to increase of entropy in the solution due to release of low charge ions (monovalent) in solution and/or increase of crystal entropy after displacement of monovalent cations by divalent cations which bound to crystal in a different manner due to their strongly held hydration shell (McBride, 1994). According to Stolz & Armbruster (2000) large divalent cations cause disorder in heulandite crystal structure. The higher charge of divalent cations compensate crystal charge deficit while actually occupying less extraframework sites. It is obvious that ion exchange among heterovalent cations is influenced by concentration-valency effect and bounds differently in crystal structure compared to monovalent cation exchange.

Radionuclides of divalent cations such as strontium or calcium are common constituents in nuclear waste materials (e.g. ⁴⁵Ca, ⁹⁰Sr). Mg, Ca, and Sr enrichment is observed in the Calico Hills Formation (clinoptilolite rich tuffs) at Yucca Mountain due to exchange reactions with

downward-percolating water. The same formations are considered potential physical barriers in case of radionuclide spillage (Vaniman *et al.*, 2001). In special conditions high irradiation doses may develop during or after adsorption of such cations, which may affect radionuclide retardation. Short-lived isotopes like ⁹⁰Sr (half life ≤ 30 yr) or other long lived isotopes like ¹³⁵Cs (half life $\leq 2.6 \times 10^6$ yr) or actinides may continue to irradiate in the zeolite structure even after the guaranteed time of 300 yr in which the storage canister may fail. In another natural example radionuclide loaded zeolites such as clinoptilolite produced from treatment of low-level sewage waters in Chernobyl were buried in shallow underground sites (Chelishchev, 1995), where continuous irradiation could affect crystal structure and subsequently retention capability. Such events increase the interest of the study of the ion exchange behaviour of zeolites for divalent cations after irradiation with various types of radiation. Hence the Oak Ridge National Laboratory, the British Nuclear Fuels, US Department of Energy Hanford Site and the Idaho National Engineering Laboratory have tested installations with zeolites for removal of ¹³⁷Cs⁺ and ⁹⁰Sr²⁺ from effluents (Mercer & Ames, 1978; Robinson *et al.*, 1995; Dyer *et al.*, 2006). In this contribution we examine the changes in ion exchange of clinoptilolite for divalent cations (Mg, Ca, Sr) after irradiation with β - and γ -radiation and attempt to relate these changes to structural changes induced by irradiation.

In the last 20 years there is increasing interest for structural changes in zeolites induced by irradiation not only for decontamination and environmental protection applications but for experimental development such as isolation of highly energetic sort lived radicals as well (Werst *et al.*, 1998). Understanding irradiation effects in solids is a major issue for environmental protection and microelectronics. Radiation catalysis is already under investigation as an advanced oxidation process (AOP) for environmental remediation (Galav *et al.*, 1997). Free radicals are generated when water is irradiated with γ -rays or electron (β -rays). These radicals effectively degrade organic compounds (*cf.* Getoff & Solar, 1986; Hilarides *et al.*, 1994; Stafford *et al.*, 1994). Application of zeolites as absorbents and catalysts in conjunction with AOP (γ -rays, β -rays) is a promising method for wastewater treatment and opens new frontiers for the understanding of applying solid catalysts in high radiation environments. Zhang *et al.* (1998) and Shkrob & Trifunac (1997) among others have reviewed the physical and chemical processes induced by radiation in zeolites and stressed the importance of zeolites in metal-to-insulator transitions, solar energy conversion and catalytic reactions. Understanding of radiation effects in micro-mesoporous solids is a critical step in elucidating and unfolding multi-phase radiolytic interactions. Such interpretations are also discussed in the present study.

Theoretical considerations

The exchange reaction between ion $A^{Z_A^+}$ (counter-ion) and ion $B^{Z_B^+}$ (co-ion) can be written as follows:



where the subscripts (c) and (s) refer to crystal and solution respectively, and Z_A , Z_B are the valences for the ions A and B respectively. M_A and N_A are the equivalent fraction of ion A in zeolite and aqueous phase respectively and they are defined by:

$$M_A = \frac{z_A m_A}{(z_A m_A + z_B m_B)} \quad (2)$$

$$N_A = \frac{z_A n_A}{(z_A n_A + z_B n_B)} \quad (3)$$

where n_A , n_B are the concentration of ions $A^{Z_A^+}$, $B^{Z_B^+}$ in solution (mol/dm^3) and m_A , m_B are the concentration of the ions in the exchanger (zeolite) (mol/kg) (Dyer *et al.*, 1981).

The rational thermodynamic equilibrium constant is defined by:

$$K_\alpha = K_m \Gamma \left(\frac{f_A^{z_B}}{f_B^{z_A}} \right) \quad (4)$$

where K_m is the mass action quotient of the ion exchange reaction (Kielland, 1935), Γ is the fraction of activity coefficients in solution and f_A , f_B are the activity coefficients of the ions in the zeolite phase (Gaines & Thomas, 1953). It is apparent from equation (4) that the calculation of the thermodynamic equilibrium constant involves two correction

factors due to departure from ideality for solution phase and for exchanger phase. Ideality is defined as the zeolite phase in homoionic form immersed in an infinitely dilute solution of the same ion (Gaines & Thomas, 1953). Equation (4) is described in detailed in Moraetis *et al.* (2007).

The preference of zeolite for one of the two cations is expressed by the corrected selectivity coefficient K_c (Kielland coefficient):

$$K_c = K_m \times \Gamma. \quad (5)$$

Plots of $\ln K_c$ vs. M_A are used to calculate the rational thermodynamic constant K_α (Eq. (6)) and the activity coefficients of the ions in the zeolite phase $f_A^{z_B}$, $f_B^{z_A}$ (Eqs. (7), (8)) (Gaines & Thomas, 1953):

$$\ln K_\alpha = (z_B - z_A) \int_0^1 \ln K_c dM_A \quad (6)$$

$$\ln f_A^{z_B} = (z_B - z_A) M_B + \ln K_c^{(M_A)} + M_A \ln K_c^{(M_A)} + \int_1^{M_A} \ln K_c dM_A \quad (7)$$

$$\ln f_B^{z_A} = -(z_B - z_A) M_A + M_A \ln K_c^{(M_A)} + \int_0^{M_A} \ln K_c dM_A. \quad (8)$$

The standard free energy per equivalent of exchange is given by:

$$\Delta G^\circ = - \frac{RT}{z_A z_B} \ln K_\alpha \quad (9)$$

where R is the gas constant and T is temperature (kelvins).

Materials and methods

Materials characterization and pretreatment

The HEU-type zeolite-rich material was collected from the Republic of Armenia (Nor Kohb deposit in Noyemberian region). It is a fine-grained silicic tuff containing 56 % HEU-type zeolite, 14 % quartz, 7 % albite, 7 % muscovite, 16 % amorphous matter and traces of smectite (Table 1). Part of the original material (sample N₀) was treated with gamma radiation in the Institute of Nuclear Chemistry CNR, Rome, Italy, and part of the sample N₀ was irradiated with β -radiation in Yerevan Institute of Physics in Armenia. Batches of irradiated material were prepared using three different doses of β -radiation 10^{12} e/cm² (sample N₁), 10^{15} e/cm² (sample N₂), 3×10^{16} e/cm² (sample N₃) and γ -radiation 70 Mrad (sample N₄) (Table 2). The quantity of sample N₃ was inadequate for a complete thermodynamic analysis. The materials were dried at 105 °C, ground in a ball mill and subsequently with pestle and mortar so as to pass from the 125- μm sieves and stored at room temperature in desiccators.

HEU-type zeolite chemistry was determined by electron microprobe analysis (EPMA) of carbon coated polished thin sections in the first part of this study (Moraetis *et al.*, 2007). Structural formulae were calculated on the basis

Table 1. Quantitative mineralogical analysis including amorphous determination by Rietveld method (relative standard deviation 5 %).

	N ₀	N ₁	N ₂	N ₃	N ₄
Clinoptilolite	56	55	55	42	56
Quartz	14	13	10	13	10
Albite	7	10	12	8	9
Mica	7	6	8	6	6
Amorphous	16	16	15	31	19

of 72 oxygen atoms, making the following assumptions: Si and Al were assigned in tetrahedral sites and Ca, Mg, Ba, Sr, K and Na are exchangeable cations. The quality of analyses was evaluated from the balance equation, $E = [Al + Fe - (2Ca + 2Mg + 2Sr + K + Na)] / [2(Ca + Mg + Ba + Sr) + K + Na]$ (Gottardi & Galli, 1985). Only those analyses with $E < \pm 10\%$ were considered reliable. The characterization of HEU-type zeolites was based on their Si:Al ratio (Meier & Olson, 1992) and on thermal stability tests after successive heating at 550 °C for 16 h (Alietti, 1972; Boles, 1972). In addition, the new classification by Bish & Boak (2001) was also considered for the characterization of our sample. According to the chemical and thermal characteristics the HEU-type zeolite is clinoptilolite (Moraetis *et al.*, 2007).

Homoionic Na-clinoptilolite was obtained by saturation of the zeolitic material with 1M NaCl solution into polypropylene bottles using a solid mass/solution volume ratio of 1/15. The bottles were kept in water bath at 70 °C and the solution was changed daily for eight days (Loizidou, 1982). Subsequently the zeolitic material was washed thoroughly until chloride free (electrical conductivity of the supernatant solution was less than 40 μ S) dried at 80 °C and stored in a desiccator.

Cation exchange capacity (CEC) of the non-irradiated clinoptilolite (N₀) was determined with three different methods:

- Saturation with 1 M KCl solution, which was changed daily, for eight days at 25 °C, followed by replacement of K⁺ with Cs⁺ using 1 M CsCl (Ming & Dixon, 1986; Ming & Boettinger, 2001) and measurement of the K⁺ index cations. CEC was determined in triplicate (denoted as method I).
- Saturation with 1N ammonium acetate solution for 10 days at 25 °C followed by distillation in a Kjeldahl microsteam distillation apparatus. During NH₄⁺-saturation the supernatant solution was replaced daily. CEC also was determined in triplicate (denoted as method II).
- Electron microprobe analysis (EPMA) of clinoptilolite crystals, which permitted calculation of the structural formulae. CEC was calculated from the CaO, MgO, SrO, BaO, Na₂O and K₂O concentrations determined by the EPMA analysis (denoted as method III). Relative error for method III is $\pm 7.67\%$ (mean of 8 analyses). The CEC obtained by method III has been defined as apparent CEC of the HEU-type crystals (Moraetis *et al.*, 2007). The term theoretical CEC adopted by Inglezakis (2005) for the CEC determined by EPMA is not considered appropriate, because microanalyses of

Table 2. Sample list with the type of irradiation and applied dose.

Sample	Radiation	Dose
N ₀	original sample no radiation applied	
N ₁	β	10 ¹² e/cm ²
N ₂	β	10 ¹⁵ e/cm ²
N ₃	β	3 × 10 ¹⁶ e/cm ²
N ₄	γ	70 Mrad

zeolites are often affected by the presence of other minerals, due to analytical constraints, such as the use of a defocused electron beam during analysis and the size of the zeolite crystals, which is often smaller than the excited area. The relative error of cation exchange value for methods I and II is $\pm 1.2\%$.

Ion exchange experiments

The ion exchange experiments were conducted at 25 °C. Initially 1N NaCl, SrCl₂, CaCl₂ and MgCl₂ stock solutions were prepared, from which batch solutions were produced. Several isotherm points were obtained by equilibrating aqueous binary mixed solutions of Sr²⁺/2Na⁺ Ca²⁺/2Na⁺ and Mg²⁺/2Na⁺ ratios with 0.2 g of Na-homoionic zeolitic material in polyethylene bottles. The normality of all solutions was 0.025 N. The suspensions were agitated and left to equilibrate for 8 days under periodic stirring. Kinetic experiments by Pabalan & Bertetti (1999) have shown that ion exchange equilibrium is approached essentially in 2–3 days. After equilibration the suspensions were centrifuged and the supernatant solutions were collected to obtain the forward points of the isotherms.

In each isotherm, several reverse points were obtained by replacing 20 cm³ of the initial suspensions with solutions of different proportion of the ion in question. The proportions of ions were selected so as to transfer a forward point with low M_A and N_A to a reverse point with high M_A and N_A value and *vice versa*. This ensured that the isotherm was reversible over the whole range of solution compositions (Loizidou, 1982). The suspensions were left 8 days to re-equilibrate, centrifuged and the supernatant solutions were analyzed (Fletcher & Townsend, 1981).

The exchange level was determined by the difference between the initial and final concentration of the different cations. Determination of Cs⁺, K⁺ and the index cation (Na⁺) was carried out with atomic absorption spectrometry (AAS) using a Perkin-Elmer AAnalyst 100 atomic absorption spectrometer. The uncertainty in the determination of Cs⁺, K⁺ and Na⁺ was 1 %, 3 % and 1 % respectively, based on the reproducibility of the measurements (3 replicates per measure). All reagents were of analytical grade (Merck).

Crystal structure refinement

Crystal structure refinement was applied to all samples (N₀, N₁, N₂, N₃, N₄) exchanged with Sr²⁺. The X-ray data were

collected in the angular range 5–80° 2 θ using a 0.03° step and counting time of 10 s per step with the same diffractometer used in bulk mineralogical analysis. All samples (N₀, N₁, N₂, N₃, N₄) were previously dried at 105 °C and were refined as polycrystalline materials without using any separation technique. The Rietveld method was applied for refinement of the polycrystalline samples, and three mineral phases (clinoptilolite, quartz, albite) were used in each sample for the refinement procedure (Bish & Post, 1989). Topas (version 3), from BRUKER, was used for Rietveld refinement, which is based on fundamental parameters (FP) algorithms, whereas background was calculated by Chebyshev polynomial algorithm. Clinoptilolite structure was refined and for quartz and albite only lattice parameters were refined. Due its low concentration in the sample we did not refine albite crystal structure. Quantitative analysis was applied for the determination of the crystalline phases and the amorphous material present in the samples and results are presented in Part I of the present study (Moraetis *et al.*, 2007). For clinoptilolite content we used the final crystal structure model after refinement by the Rietveld method. For the amorphous determination, a known amount of corundum was added (Hill & Howard, 1987; Bish & Howard, 1988). The refinement progress was checked by the statistical parameters R_p and GooF, which depict the quality of the fitting for the XRD pattern and the rationality of the selected fitting procedure respectively. Moreover the precision of the quantitative mineralogical analyses is $\pm 5\%$.

Refinement was initially started in $C2/m$ space group, as in Part I with Cs-saturated clinoptilolite, following the reasoning of Stolz & Armbruster (2000). However in our case $C2/m$ yielded poor refinement results, thus the Cm space group was applied for Sr²⁺ saturated heulandite (Dobelin & Armbruster, 2003 – Inorganic Crystal Structure Database No. 96825). Tetrahedral coordinates were kept constant, whereas the scale factor and lattice parameters were refined in each cycle. Cation coordinates and site occupancy for extra framework positions also were refined in separate cycles. In this point we make clear that tetrahedral framework was not refined since to many parameters had to be included and sample constrains (multiphase polycrystalline material) did not allow such action, since we would not be sure if the observed changes in zeolite partial refinement would be influenced, by the presence of the no zeolitic contribution to the diffractogram or due to radiation effects in zeolites. In addition for the same aforementioned reasons, we would not be able to identify sound differences in bond distances as Dobelin & Armbruster (2003) did between Al-O and Si-O (*i.e.* 0.06 Å).

Results

Material characterization

The average chemical composition (mean of 8 analyses) and the formulae on the basis of 72 oxygens of clinoptilolite crystals obtained by EPMA are given in Moraetis *et al.* (2007). The average structural formulae is (K_{0.34}

Na_{0.93} Mg_{0.41} Ca_{2.12}) [Al_{6.82} Si_{29.32} O₇₂]-H₂O. According to Coombs *et al.* (1998) the HEU-type material is clinoptilolite because the Si⁴⁺/Al³⁺ ratio is greater than 4. In addition, in the classification scheme of Bish & Boak (2001) which takes into consideration compositional variation of the extraframeworks, our sample is projected in the region where clearly clinoptilolites are presented (Ca + Mg + K + Na = 3.8, Al + Fe = 6.82). Chemical analyses of the whole rock have shown that the parent tuff had silicic affinities (Moraetis *et al.*, 2007) in accordance with the results of Petrosov & Sadoyan (1998) and Petrosov & Jarbashian (1999). The modal mineralogical composition of the original and irradiated samples is shown in Table 1. The main difference observed is the decrease of clinoptilolite content and increase of amorphous material in sample N₃ compared to other samples.

The CEC determined by methods I, II and III and the relative errors respectively are identical with those presented by Moraetis *et al.* (2007). However, sample N₁ exhibited small difference in the normalized CEC value and this due to different clinoptilolite content determined in this study (55 %) compared to the value determined by Moraetis *et al.* (2007) (56 %). The aforementioned difference in clinoptilolite content lies within the method's uncertainty.

The presence of other phases such as quartz (10–13 %), albite (7–12 %), mica (6–7 %) and amorphous matter (16 %) may contribute partly to the total CEC determined in this study. Illite has CEC 0.1–0.4 meq/g which contributes 0.014–0.03 meq/g after normalization to 7 % content and quartz and albite do not have CEC. Moreover Hepper *et al.* (2006) found that the presence of 85 % amorphous matter in a soil contributed to the CEC up to 0.09 meq/g, which corresponds to 0.014 meq/g in the present study after normalization to 16 % content. Considering the maximum CEC values from the preceding calculations for each phase we end up with a total of ± 0.05 meq/g which is well within the range of standard error calculated for the CEC of clinoptilolite, *i.e.* ± 0.12 – 0.17 meq/g (Moraetis *et al.*, 2007).

Ion exchange isotherms and thermodynamic parameters

The ion exchange isotherms for the binary systems Sr²⁺ \leftrightarrow 2Na⁺, Ca²⁺ \leftrightarrow 2Na⁺ and Mg²⁺ \leftrightarrow 2Na⁺ containing forward and reverse points are shown in Fig. 1–3 respectively. The ion exchange isotherms are plots of the equilibrium equivalent mole fraction of an exchanging ion in solution *vs.* the equilibrium equivalent mole fraction of the same ion in clinoptilolite. The best fitted curve was applied to isotherm points by curvilinear regression analysis. The equilibrium concentrations of each cation in clinoptilolite, M_A , and the solution, N_A , were calculated from the concentrations of both cations involved in each ion exchange system. Also, sample weight, solution volume and CEC were involved in the calculation of cationic mole fractions. The equations used to calculate the cationic mole fraction of an

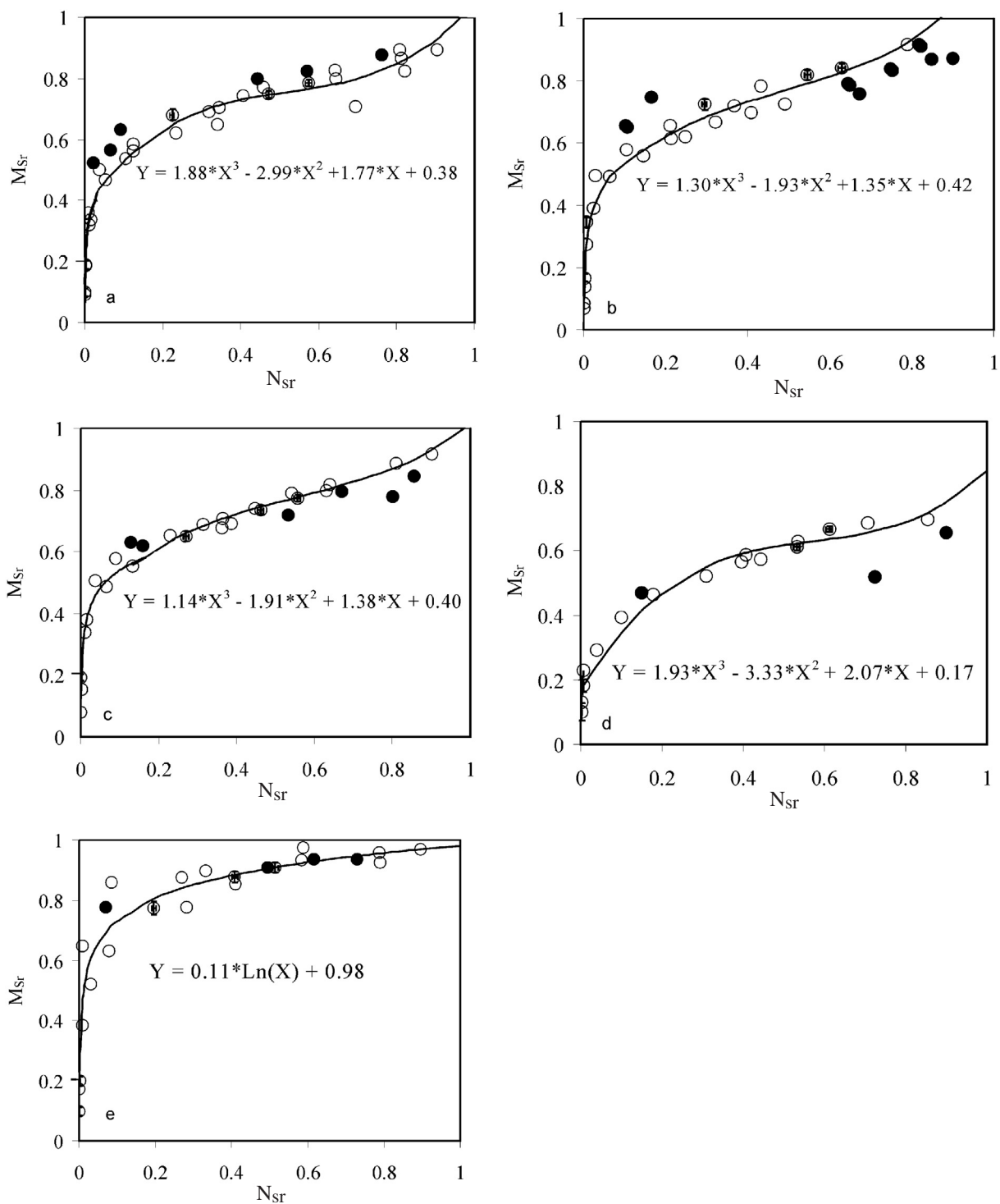


Fig. 1. Isotherms for ion exchange $\text{Sr}^{2+} \leftrightarrow 2\text{Na}^+$ at 25 °C with constant normality 0.025N. Empty circles correspond to forward points and full circles to reverse points. (a) sample N0, (b) sample N1, (c) sample N2, (d) sample N3 (e) sample N4. Fit equations and error bars are presented.

ion in the zeolite and solution are the following:

$$M_A = \frac{(X_i - X_f \times V)}{(X_i - X_f \times V) + (CEC \bullet W - Na_f \times V + Na_i)} \quad (10)$$

$$N_A = \frac{X_f}{X_f + Na_f} \quad (11)$$

where, X_i , X_f are the initial and final concentration, respectively, of the cation in question in solution (Sr^{2+} , Ca^{2+} and Mg^{2+}), and Na_i and Na_f are the initial and final concentration, respectively, of Na^+ in solution. CEC is the cation exchange capacity for each sample. W and V are the sample weight (g) and the solution volume (ml) respectively. The error bars in selected points in the isotherm lines were calculated by the following equation (12):

$$U_r^2 = \left(\frac{\partial r}{\partial x_1}\right) U_{x_1}^2 + \left(\frac{\partial r}{\partial x_2}\right) U_{x_2}^2 + \dots + \left(\frac{\partial r}{\partial x_j}\right) U_{x_j}^2 \quad (12)$$

where U_r is the result uncertainty, U_{x_i} is the uncertainty in the measured variables, r is the result and x_1 is the measured variable (*e.g.* weight, solution volume, concentration, *etc.*) (Coleman & Steele, 1999). The standard error calculated was 0.01–0.03. However the relative error was 1.5 % to 25 % in the extrema of the isotherm line in accordance with previous workers (*e.g.* Pabalan, 1994). The large relative errors in the isotherm extrema are attributed to error in determination of the incoming and/or outgoing ion at low solution concentrations.

The isotherm curves for $Sr^{2+} \leftrightarrow 2Na^+$ and $Mg^{2+} \leftrightarrow 2Na^+$ binary systems were best fitted by 3rd order polynomial equations. In contrast, the $Ca^{2+} \leftrightarrow 2Na^+$ system was not adequately fitted either by polynomial or by logarithmic equation, moreover the upper part of the isotherm ($N_{Ca} > 0.34$) was rather linear whereas the lower part was fitted to a logarithmic curve. The coefficient of determination (R^2) varied between 0.93 and 0.98 for all isotherms. The isotherm for the binary system $Sr^{2+} \leftrightarrow 2Na^+$ and samples N_0 N_1 N_2 N_3 is sigmoidal and according to Colella (1996) it is a type-c isotherm (Fig. 1). Similar observations were made by Pabalan & Bertetti (1999) for natural clinoptilolite and were attributed to successive filling by Sr^{2+} , initially of the highly preferred sites (*i.e.* low concentration of Sr^{2+} in solution), subsequently of the less preferred sites (*i.e.* inversion area in isotherm line) and finally of sites where Na^+ is more preferable compared to Sr^{2+} (*i.e.* last part of the isotherm line-high Sr^{2+} concentration in solution). The isotherm of sample N_4 exhibits preference for Sr^{2+} and is classified as type-b according to Colella (1996) or as type-a according to Breck (1974) (Fig. 1). In samples N_0 , N_1 , N_2 and N_3 , the lower part of the isotherm (N_{Sr} 0–0.05) was fitted with a logarithmic equation so as to obtain isotherm data for thermodynamic calculations. In samples N_0 , N_1 and N_4 , the isotherms of the system $Ca^{2+} \leftrightarrow 2Na^+$ were fitted with a logarithmic equation for $M_{Ca} \leq 0.68$ and with a polynomial or a power type curve for higher M_{Ca} values (Fig. 2). This shows that selectivity for Ca^{2+} increases at low Ca^{2+} solution concentrations decreasing thereafter. In contrast, the isotherm of sample N_2 exhibits an increased Ca^{2+} selectivity even for M_{Ca} higher than 0.66

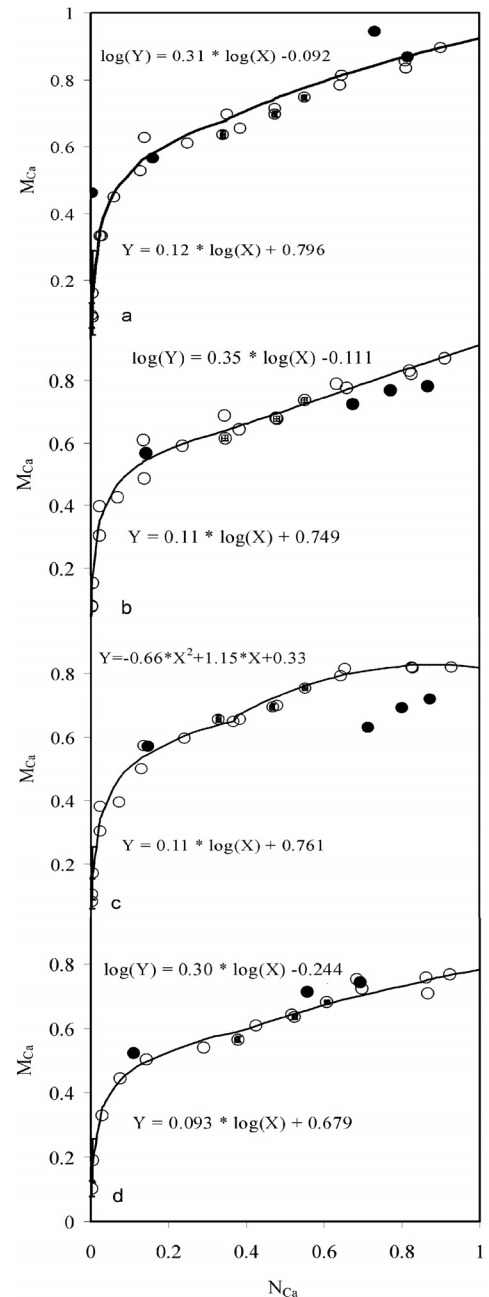


Fig. 2. Isotherms for ion exchange $Ca^{2+} \leftrightarrow 2Na^+$ at 25 °C with constant normality 0.025N. Empty circles correspond to forward points and full circles to reverse points. (a) sample N_0 , (b) sample N_1 , (c) sample N_2 , (d) sample N_4 . Fit equations and error bars are presented. Fit equations for M_{Ca} for higher and lower values of 0.65 are depicted in upper and lower part of the isotherm graph respectively.

and shows hysteresis for M_{Ca} 0.66–0.8 (f-type isotherm after Colella, 1996). Isotherms presented by Pabalan (1994) for the $Ca^{2+} \leftrightarrow 2Na^+$ exchange and 0.05 N solutions are comparable to the present study for sample N_0 . Finally the isotherms for the binary system $Mg^{2+} \leftrightarrow 2Na^+$ were best fitted by 3rd order polynomial equations. The sigmoidal shape was preserved for all isotherms. There is a slight preference for Mg^{2+} for M_{Mg} up to 0.3, but at higher M_{Mg}

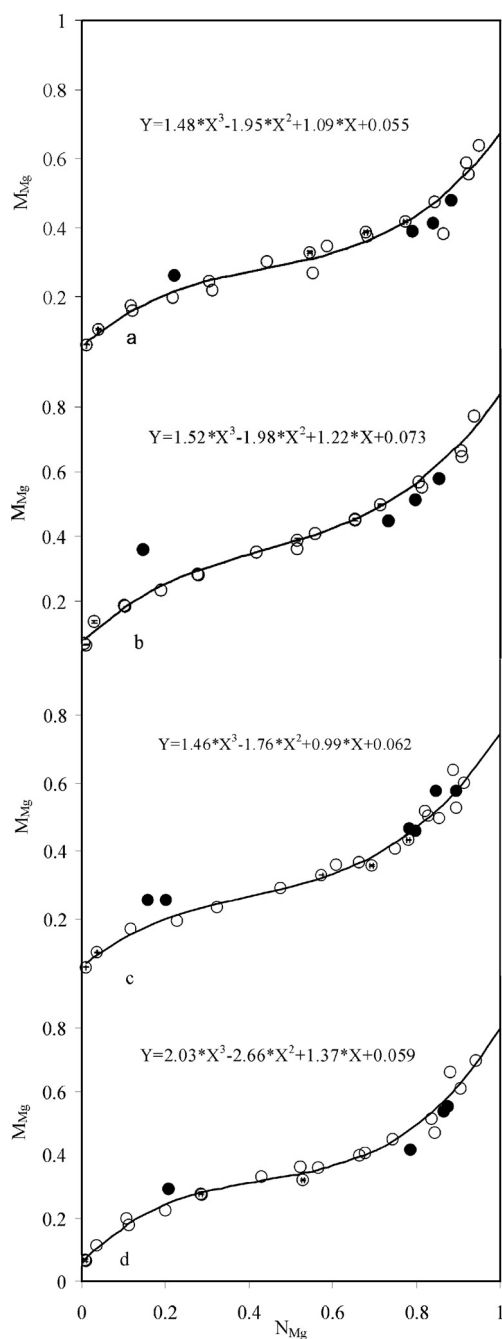


Fig. 3. Isotherms for ion exchange $\text{Mg}^{2+} \leftrightarrow 2\text{Na}^+$ at 25 °C with constant normality 0.025N. Empty circles correspond to forward points and full circles to reverse points. (a) sample N0, (b) sample N1, (c) sample N2, (d) sample N4. Error bars are presented.

values a selectivity reversal is observed. Sample N₂ displays an increase in selectivity for Mg^{2+} compared to sample N₀.

The activity ratio Γ varied from 0.91 to 1.08. The electrolyte mean activity coefficient for each salt in pure state was calculated by the extended Debye & Hückel equation simplified by Guntelberg (1926) ($\log \gamma_{\pm AX} = \frac{-A|z_A z_X| \sqrt{I}}{1 + \sqrt{I}}$). Truesdell-Jones equation was tested for univalent-univalent

exchange but yielded similar results as already mentioned in Moraetis *et al.* (2007). However Truesdell-Jones equation was tested also for univalent-bivalent exchange and the results for Gibbs free energy (ΔG°) for $\text{Mg}^{2+} \leftrightarrow 2\text{Na}^+$ was identical (9.86 kJ/mole) and for $\text{Ca}^{2+} \leftrightarrow 2\text{Na}^+$ was lower (3.66 kJ/mole). Guntelberg equation yielded K_α and ΔG values closer to those obtained by Pabalan & Bertetti (1999), *i.e.* 3.74 kJ/mole for the binary system $\text{Ca}^{2+} \leftrightarrow 2\text{Na}^+$, whereas Pabalan & Bertetti (1999) yielded 4.09 ± 0.20 kJ/mole. The observed difference is within experimental error (0.09–0.2 kJ/mole) calculated in the present study and thus Guntelberg equation was selected. In addition, small differences in Gibbs free energy may also be attributed to physical factors (Langella *et al.*, 2000; Cerri *et al.*, 2002).

The Kielland plots for all samples in the three binary systems are shown in Fig. 4 ($\text{Sr}^{2+} \leftrightarrow 2\text{Na}^+$), Fig. 5 ($\text{Ca}^{2+} \leftrightarrow 2\text{Na}^+$) and Fig. 6 ($\text{Mg}^{2+} \leftrightarrow 2\text{Na}^+$). Kielland plots for the binary system $\text{Sr}^{2+} \leftrightarrow 2\text{Na}^+$ were modelled by linear equations except for samples N₃ and N₄ which were best fitted with a 3rd order polynomial and a quadratic equation respectively. The $\text{Ca}^{2+} \leftrightarrow 2\text{Na}^+$ plots were best fitted with a quadratic equation, whereas the $\text{Mg}^{2+} \leftrightarrow 2\text{Na}^+$ plots were best fitted with 3rd order equations. In all samples the selectivity coefficient (Kielland plots) decreased with increase of the equivalent fraction in clinoptilolite. This is expected since the exchangeable sites are progressively filled as the equivalent fraction in clinoptilolite increases. The Kielland plots in the $\text{Sr}^{2+} \leftrightarrow 2\text{Na}^+$ system show major changes in samples N₃ and N₄ compared to N₀ and this is confirmed by the change of the regression line from linear (sample N₀) to polynomial and quadratic respectively. Such changes are probably related with changes in site selectivity and formation or elimination of certain exchange sites (see below). The regression lines of Kielland plots in $\text{Ca}^{2+} \leftrightarrow 2\text{Na}^+$ systems do not change in the examined samples. However changes in quadratic equation coefficients for sample N₂ indicate change in Gibbs free energy and increase in Ca^{2+} selectivity, probably due to increase in accessibility for certain exchange sites. Kielland plots in $\text{Mg}^{2+} \leftrightarrow 2\text{Na}^+$ systems remain unchanged, suggesting lack of major structural changes after irradiation.

The rational equilibrium constant K_α and Gibbs free energy ΔG° of exchange at standard state were calculated by integration of Kielland plots and the results are listed in Table 3. Sample N₀ exhibits the following selectivity order $\text{Sr} > \text{Ca} > \text{Mg}$ in accordance with previous reports (Ames, 1960, 1961). Samples N₁ and especially N₂ exhibit higher selectivity for all ions compared to sample N₀, corroborating the isotherm data. Sample N₄ shows remarkable increase in Sr^{2+} selectivity in accordance to the observed change in isotherm shape and lower selectivity for Mg^{2+} compared to N₀ (Fig. 1 and 3), whereas the selectivity for Ca^{2+} remains unchanged (Fig. 2).

The activity coefficients in the exchanger for the $\text{Sr}^{2+} \leftrightarrow 2\text{Na}^+$, $\text{Ca}^{2+} \leftrightarrow 2\text{Na}^+$ and $\text{Mg}^{2+} \leftrightarrow 2\text{Na}^+$ systems are shown in Fig. 7–9 respectively. $\text{Sr}^{2+} \leftrightarrow 2\text{Na}^+$ exchange is characterized by similar activity coefficient plots in samples N₀ and N₁. In contrast, N₂ exhibits a slight different activity coefficient plot and samples N₃ and N₄ show major

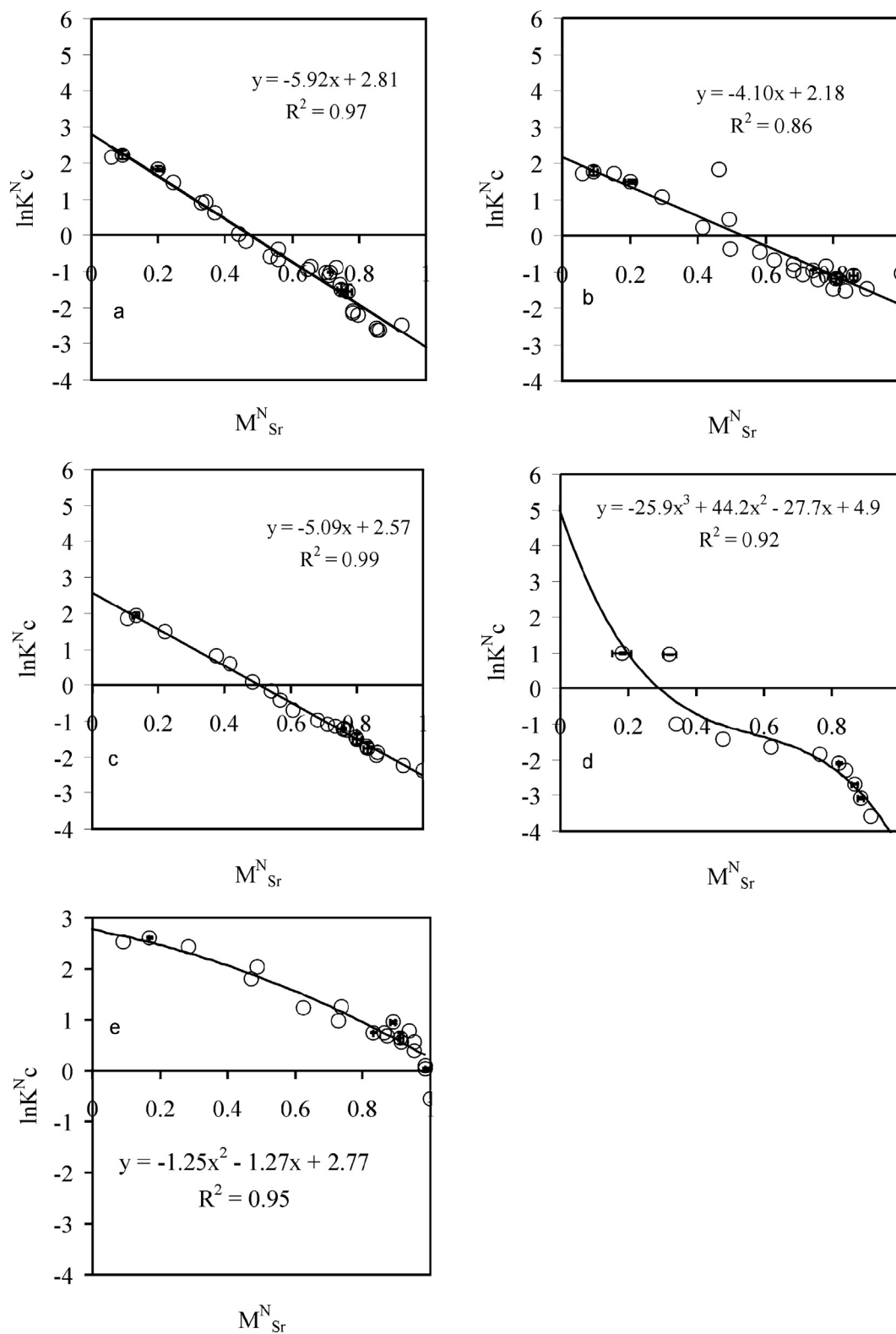


Fig. 4. Normalized Kielland plots for $Sr^{2+} \leftrightarrow 2Na^+$ exchange against equivalent fraction of Sr^{2+} in the original and irradiated clinoptilolite. (a) N0, (b) N1, (c) N2, (d) N3, (e) N4. Best fit curve and curve equation was determined by regression analysis.

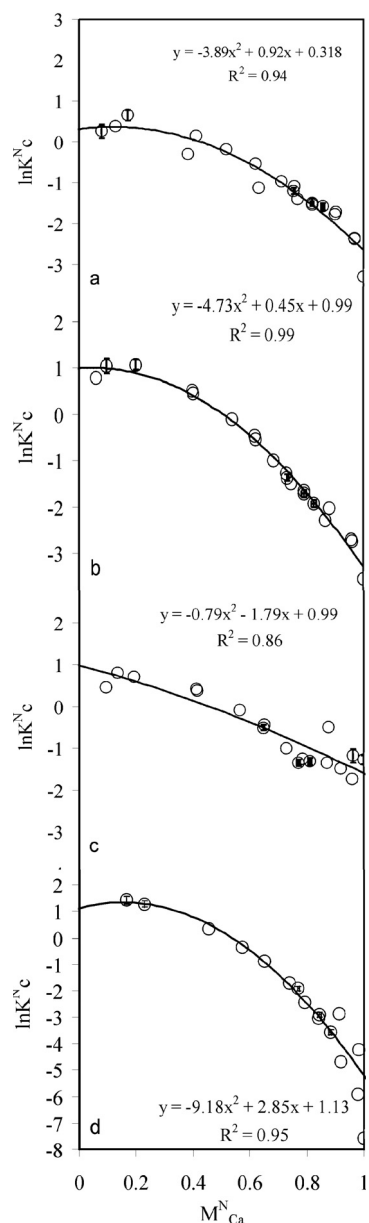


Fig. 5. Normalized Kielland plot for $\text{Ca}^{2+} \leftrightarrow 2\text{Na}^+$ exchange against the normalized equivalent fraction of Ca^{2+} in the original and irradiated clinoptilolite. (a) N0, (b) N1, (c) N2, (d) N4. Best fit curve and curve equation was determined by regression analysis.

differences compared to sample N₀. The activity coefficient plot of N₃ exhibits a large area whereby both activity coefficients for the incoming and the outgoing ion are equal, suggesting that a concentration range exists in which both ions exhibit simultaneously equal activity coefficients. It is inferred that the two ions segregate in different sites not influenced by each other. A similar assumption can be made for sample N₄, in which the activity coefficient of the incoming ion increases sharply, whereas the activity coefficient of the outgoing ion decreases slightly. This implies that the outgoing ion is not severely affected by the increased site occupancy of the incoming ion. The activity coefficient plot for $\text{Ca}^{2+} \leftrightarrow 2\text{Na}^+$ exchange in sample N₀

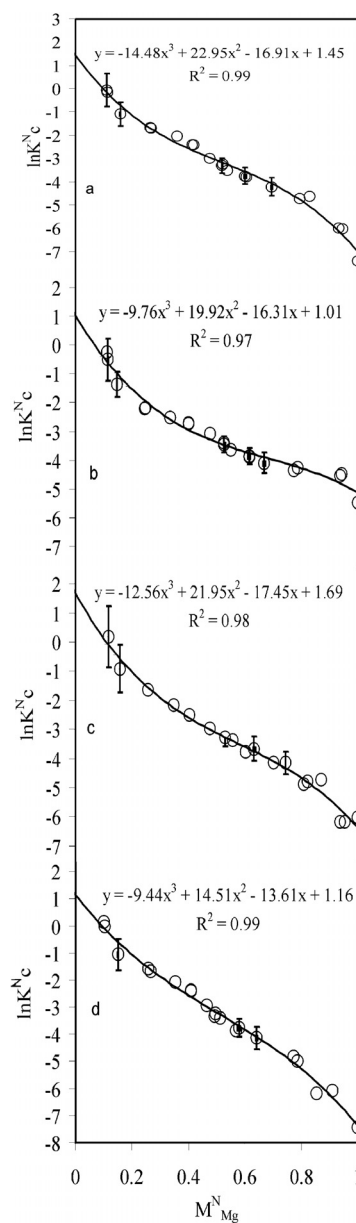


Fig. 6. Normalized Kielland plot for $\text{Mg}^{2+} \leftrightarrow 2\text{Na}^+$ exchange against the normalized equivalent fraction of Ca^{2+} in the original and irradiated clinoptilolite. (a) N0, (b) N1, (c) N2, (d) N4. Best fit curve and curve equation was determined by regression analysis.

is different compared to the activated samples N₁, N₂ and N₄. This is probably related to modified exchangeable sites caused by structural changes after radiation. In particular, the activity coefficient plot of sample N₂ is remarkably different compared to N₀. Moreover the activity coefficient of Ca^{2+} initially decreases and then increases to a maximum followed by a slight decrease. Such behaviour is related with the sites occupied by Ca^{2+} and the probable inability of Ca^{2+} to approach Na^+ sites. The $\text{Mg}^{2+} \leftrightarrow 2\text{Na}^+$ system exhibits similar activity coefficient plots for all samples. As the equivalent fraction of the incoming divalent cation increases, minima and maxima are observed for sodium and the incoming divalent cation respectively. The minima and

Table 3. Thermodynamic results for exchange $\text{Sr}^{2+} \leftrightarrow 2\text{Na}^+$, $\text{Ca}^{2+} \leftrightarrow 2\text{Na}^+$, $\text{Mg}^{2+} \leftrightarrow 2\text{Na}^+$ for the samples $\text{N}_0, \text{N}_1, \text{N}_2, \text{N}_3, \text{N}_4$.

Samples	$\ln K\alpha$ at 298 K	ΔG° (kJ/mole)
$\text{Sr}^{2+} \leftrightarrow 2\text{Na}^+$		
N_0	-1.15	2.85
N_1	-0.97	2.40
N_2	-0.97	2.41
N_3	-1.65	4.09
N_4	0.72	-1.78
$\text{Ca}^{2+} \leftrightarrow 2\text{Na}^+$		
N_0	-1.51	3.74
N_1	-1.36	3.38
N_2	-1.17	2.90
N_4	-1.51	3.74
$\text{Mg}^{2+} \leftrightarrow 2\text{Na}^+$		
N_0	-3.98	9.86
N_1	-3.94	9.75
N_2	-3.86	9.57
N_4	-4.17	10.32

maxima in activity coefficients are expected due to replacement of the outgoing monovalent cations by the incoming divalent cations in exchangeable sites.

Structure refinement of the Sr-exchanged samples

As already mentioned crystal structure was refined in Cm space group. Dobelin & Armbruster (2003) attributed the lowering of symmetry to Al accumulation in tetrahedral T2 which is also reflected in Sr extraframework sites. As in part I, Si and Al tetrahedral positions were not refined and Dobelin & Armbruster coordinates were applied. Refinement of Sr extraframework positions exhibited statistically sound results in Cm space group.

The crystallographic parameters for samples $\text{N}_0, \text{N}_1, \text{N}_2, \text{N}_3$ and N_4 , are listed in Table 4. Table 5 shows the refinement results for Sr^{2+} extraframework sites. Lattice parameters remain unchanged in the irradiated ($\text{N}_1, \text{N}_2, \text{N}_3, \text{N}_4$) and non-irradiated (N_0) samples. The statistical values R_p and GooF in Rietveld refinement indicate a good agreement between the theoretical and calculated intensity values. The differences in statistical values between the refinement of Dobelin & Armbruster (2003) and the present study are mainly due to the lower accuracy observed in polycrystalline crystal refinements compared to single-crystal structure refinement.

Although the extraframework Sr sites in sample N_0 (Fig. 10) resemble to those of the experimental model of Dobelin & Armbruster (2003), different occupancies of the sites are observed. Occupancies in the present study are lower than expected due to the higher Si/Al ratio. In addition, differences in extraframework site coordinates between the initial model and sample N_0 can be attributed also to the Si/Al ratio, because attractive forces between cations and framework oxygens depend on the ratio of substitution of silicon by aluminium. Moreover site Sr4 is not

occupied by Sr^{2+} and this is in accordance with Dobelin & Armbruster (2003) observations for the satellite position Sr4. Irradiated samples $\text{N}_1, \text{N}_2, \text{N}_3$ and N_4 exhibit changes in coordinates and occupancy of sites Sr1, Sr2 and Sr3 compared to sample N_0 . In samples N_2 and N_3 , a shift of site position Sr1 along a axis by 1.768 Å and 1.265 Å respectively is observed. Furthermore, the same samples exhibit a shift of site Sr1 along c -axis by 1.112 Å and 0.708 Å respectively towards the clinoptilolite tetrahedra (Table 5). Occupancy for Sr1 site remains constant in samples N_1, N_2 , and decreases for samples N_3 and N_4 . Site Sr3 is generally unaffected by irradiation except for sample N_3 which exhibits a shift along a -axis and c -axis by 1.841 Å and 1.057 Å respectively towards the clinoptilolite channel centre (Table 5). The coordinates of site Sr2 remain unchanged, although their occupancy decrease for samples irradiated with β -radiation. Finally site Sr3 exhibits a slight increase in occupancy for samples irradiated with β - and γ -radiation. In summary, Rietveld refinement suggests that after irradiation sites S1 and S3 shift towards the wall of channel A and the centre of channel B respectively and the occupancy of Sr^{2+} sites changes.

Discussion

Ion exchange and thermodynamic parameters

Determination of the correct CEC is of major importance because it is used for thermodynamic calculations and normalization of isotherm data. Detailed discussion of CEC calculations has been presented by Moraetis *et al.* (2007). 2.43 meq/g is the CEC obtained by methods I and II and it is within the range of CEC values reported for clinoptilolite in other studies. Langella *et al.* (2000) reported CEC for clinoptilolite 2.66 meq/g which is greater than the present study and this can be justified by the lower ratio of $\text{Si}^{4+}/\text{Al}^{3+}$ (4.17) compared to the present study ($\text{Si}^{4+}/\text{Al}^{3+}$ ratio 4.3). All samples including N_3 have the same CEC after normalization to 100 % clinoptilolite (Moraetis *et al.*, 2007).

The influence of β -radiation on univalent ion exchange has been already presented in Part I of this study (Moraetis *et al.*, 2007). $\text{Cs}^+ \leftrightarrow \text{Na}^+$ exchange was facilitated by β -radiation, whereas $\text{K}^+ \leftrightarrow \text{Na}^+$ exchange was not affected by β -radiation. In the present study, although β -radiation influences the $\text{Sr}^{2+} \leftrightarrow 2\text{Na}^+$ exchange by increasing the selectivity of clinoptilolite for Sr^{2+} (samples N_1 and N_2), the selectivity for Sr^{2+} decreases in N_3 . Moreover N_2 sample exhibits higher selectivity for Ca^{2+} compared to Sr^{2+} , but only a slight increase in selectivity for Mg^{2+} . The selectivity changes for both monovalent and divalent cations are not exclusively related to ionic radius. Instead specific changes in exchangeable site are probably the main factor affecting ion exchange after irradiation with β -radiation as already mentioned in Part I of this study. Similar to the univalent cations, ion exchange with divalent cations was influenced by γ -radiation and clinoptilolite selectivity for Sr^{2+} increased, for Mg^{2+} decreased and for

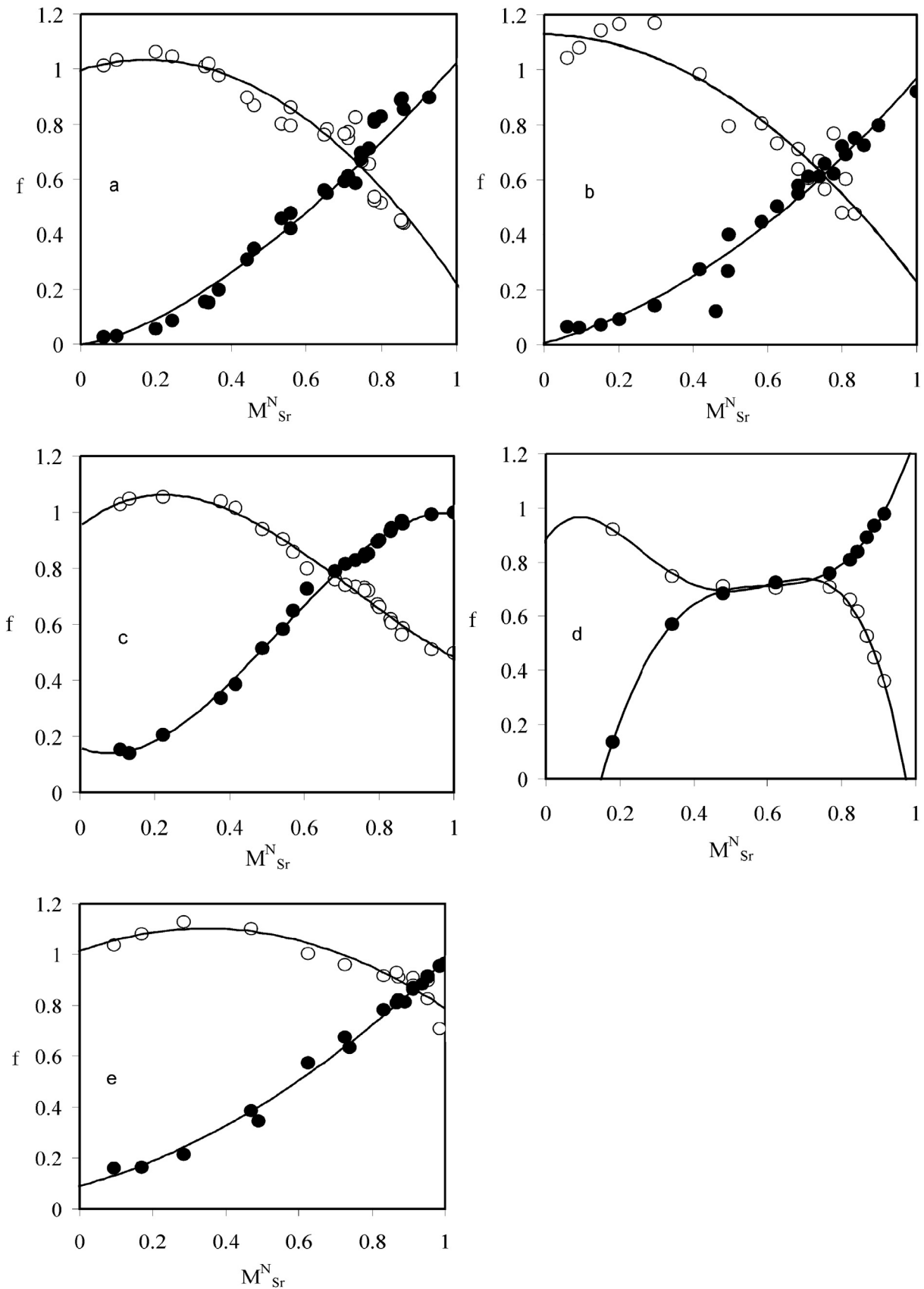


Fig. 7. Activity coefficients of Sr^{2+} (●) and Na^+ (○) in zeolite phase over equivalent fraction (normalized) of Sr^{2+} in the original and irradiated clinoptilolite. (a) N0, (b) N1, (c) N2, (d) N3 (e) N4. Gaines & Thomas (1953) equations applied.

Table 4. Lattice refinement parameters for Sr²⁺-loaded samples.

Samples	<i>a</i> (Å)	<i>b</i> (Å)	<i>c</i> (Å)	β (°)	<i>V</i> (Å ³)	Goof ^a	R _p ^b
Sr ²⁺ -exchanged samples							
Th. model							
(96825)	17.714	18.000	7.430	116.62	2117.82	1.01	3.83
N ₀	17.669(52)	17.948(59)	7.408(23)	116.47(25)	2103.1(12)	4.58	14.23
N ₁	17.677(58)	17.952(65)	7.416(25)	116.51(27)	2106.0(13)	4.40	13.78
N ₂	17.706(50)	17.974(54)	7.423(21)	116.53(24)	2113.8(11)	4.07	12.56
N ₃	17.706(51)	17.954(60)	7.423(26)	116.50(27)	2111.9(13)	3.01	9.89
N ₄	17.705(50)	17.962(54)	7.416(21)	116.47(22)	2111.2(11)	3.90	12.25

$${}^a\text{Goof} = \sqrt{\left[\frac{\sum w_i (Y_{io}^2 - Y_{ic}^2)^2}{(n - p)} \right]}.$$

n: number of measurement (X-ray intensities), *p*: number of variables in the model.

$${}^bR_p = \sum |Y_{io} - Y_{ic}| / \sum Y_{io}.$$

Y_{io} and *Y_{ic}* are the experimental and the calculated intensity for each diffraction peak. *w_i* is the relative standard deviation for each refined peak.

Table 5. Refinement results for the cation exchange positions and occupancy (standard deviations in parentheses).

Cation position	<i>x</i>	<i>y</i>	<i>z</i>	occ
Th. model (96825)				
Sr1	0.1502	0.0000	0.6789	0.759
Sr2	0.8536	0.0000	0.3437	0.457
Sr3	0.4661	0.0000	0.8124	0.780
Sr4	0.477	0.0000	0.752	0.120
N ₀				
Sr1	0.1087(34)	0.0000	0.5424(83)	0.450(39)
Sr2	0.8466(28)	0.0000	0.3209(65)	0.644(38)
Sr3	0.4346(42)	0.0000	0.7803(66)	0.430(25)
Sr4	0.477	0.0000	0.752	0
N ₁				
Sr1	0.1954(36)	0.0000	0.6935(86)	0.456(29)
Sr2	0.8897(26)	0.0000	0.4003(69)	0.550(28)
Sr3	0.4468(34)	0.0000	0.7857(60)	0.560(28)
Sr4	0.477	0.0000	0.752	0
N ₂				
Sr1	0.2088(32)	0.0000	0.6926(70)	0.454(28)
Sr2	0.8795(24)	0.0000	0.3540(55)	0.558(23)
Sr3	0.4500(25)	0.0000	0.7864(46)	0.651(23)
Sr4	0.477	0.0000	0.752	0
N ₃				
Sr1	0.1803(87)	0.0000	0.6380(19)	0.214(30)
Sr2	0.8929(41)	0.0000	0.6376(62)	0.381(27)
Sr3	0.5388(29)	0.0000	0.6376(62)	0.618(27)
Sr4	0.477	0.0000	0.752	0
N ₄				
Sr1	0.1260(62)	0.0000	0.5680(15)	0.236(33)
Sr2	0.8506(24)	0.0000	0.3201(53)	0.689(37)
Sr3	0.4538(29)	0.0000	0.7881(51)	0.553(23)
Sr4	0.477	0.0000	0.752	0

Ca²⁺ remained unchanged. Hence the observed change in selectivity of clinoptilolite irradiated with γ-radiation was controlled by the ionic radius of the three divalent cations, decreasing with decrease of ionic radius of the incoming cation. It is interesting that the opposite trend was observed in exchange of univalent cations, since clinoptilolite displayed a greater increase in selectivity for K⁺ compared to Cs⁺ (Moraetis *et al.*, 2007).

Ion exchange for all binary systems is facilitated after irradiation with β-radiation except for Sr²⁺ exchange in sample N₃, as is indicated by the decrease of Δ*G*[°] (Table 3). Hence Sr²⁺ exchange is facilitated by β-radiation between 10¹⁵ e/cm² and 3 × 10¹⁶ e/cm². A high irradiation dose like 3 × 10¹⁶ e/cm² affects adversely Sr²⁺ exchange and clinoptilolite selectivity for Sr²⁺ decreases. In sample N₂ the Gibbs free energy change is greater for the

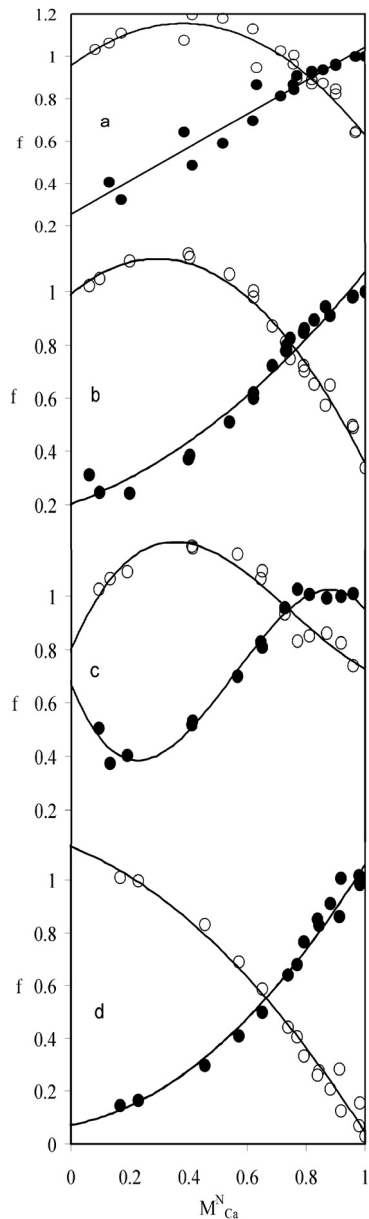


Fig. 8. Activity coefficients of Ca^{2+} (●) and Na^+ (○) in zeolite phase over equivalent fraction (normalized) of Ca^{2+} in the original and irradiated clinoptilolite. (a) N0, (b) N1, (c) N2, (d) N4. Gaines & Thomas (1953) equations applied.

system $\text{Ca}^{2+} \leftrightarrow 2\text{Na}^+$ compared to $\text{Mg}^{2+} \leftrightarrow 2\text{Na}^+$ (e.g. 0.84 kJ/mole and 0.29 kJ/mole respectively). According to Palmer & Gunter (2001) the hydration radii controls the affinity of natural clinoptilolite for certain cations. The larger the incoming cation radius the smaller the hydration shell and the higher the clinoptilolite affinity, as was confirmed by the affinity series of divalent cations presented by other workers (Ames, 1961; Chelishchev *et al.*, 1973) and was observed in this study (sample N_0). However, the decrease of ionic radius successively from Sr^{2+} to Ca^{2+} and Mg^{2+} is not correlated with the thermodynamic parameters calculated for irradiated samples in the

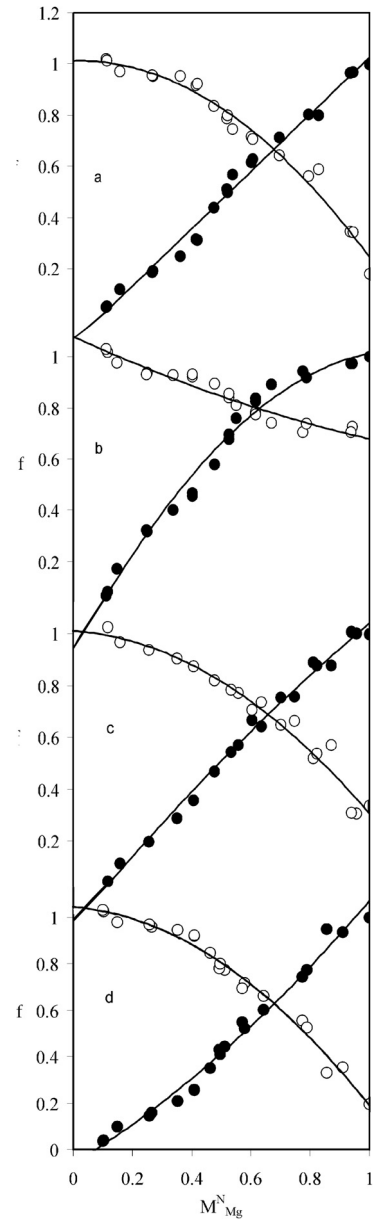


Fig. 9. Activity coefficients of Mg^{2+} (●) and Na^+ (○) in zeolite phase over equivalent fraction (normalized) of Mg^{2+} in the original and irradiated clinoptilolite. (a) N0, (b) N1, (c) N2, (d) N4. Gaines & Thomas (1953) equations applied.

binary system $\text{Ca}^{2+} \leftrightarrow 2\text{Na}^+$. The changes introduced in clinoptilolite structure by β -radiation have different impact in ion exchange of different cations, suggesting that different cationic radius is not the sole factor affecting such reaction in irradiated clinoptilolite.

The changes introduced in clinoptilolite structure by β -radiation have greater influence in exchange of univalent cation such as Cs^+ as is indicated by the change in ΔG° (Moraetis *et al.*, 2007). Divalent cations hold their hydration shell tighter than univalent cations (Palmer & Gunter, 2001) and thus the latter are easier to migrate into channels and fit into exchangeable sites. Had radiation gener-

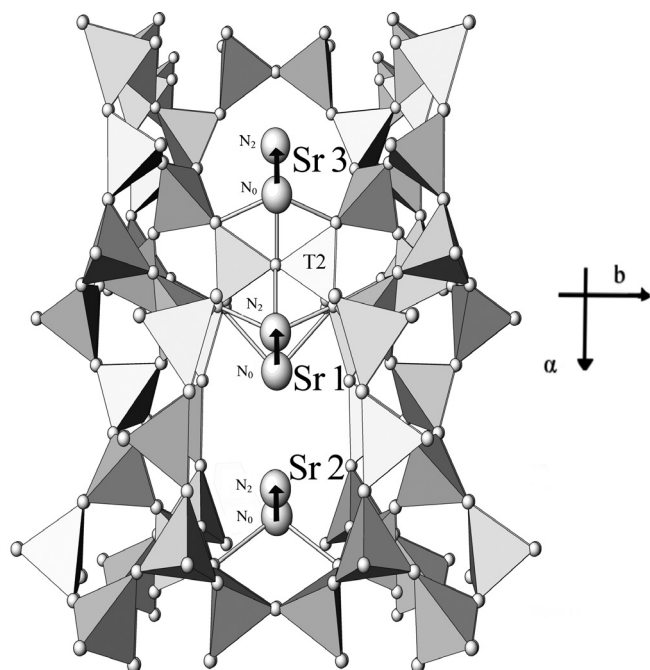


Fig. 10. Schematic representation of the clinoptilolite channels with the location of the various exchange sites before irradiation (N₀), after irradiation (N₂) and the T2 site. Projection along (001).

ated free space into channels, univalent cations would be more favoured compared to divalent cations because hydration shells can be stripped off easier. This is verified for cations like Cs⁺, Sr²⁺, Ca²⁺, Mg²⁺, since the increase of ionic potential from Cs⁺ to Mg²⁺ is generally inversely related to increase of affinity after β -radiation (Moraetis *et al.*, 2007). However K⁺ \leftrightarrow Na⁺ exchange is not affected by β -radiation (Moraetis *et al.*, 2007) and Ca²⁺ exchange exhibit greater change in ΔG° after irradiation with β -radiation compared to Sr²⁺. It has already been mentioned that other factors, except for the ionic potential, may be decisive in ion exchange after irradiation with β -radiation, such as structural changes in sites which preferably host K⁺ and Ca²⁺ as will be discussed below.

Irradiation of clinoptilolite with γ -radiation increases remarkably affinity for Sr²⁺ and decreases its affinity for Mg²⁺. In contrast, clinoptilolite affinity for Ca²⁺ after γ -radiation remained unchanged. Isotherm shapes for the binary system Sr²⁺ \leftrightarrow 2Na⁺ and sample N₄ change from *c*-type to *b*-type following Colella (1996) or to *a*-type according to Breck (1974) suggesting major changes in diffusion of Sr²⁺ within the clinoptilolite channels. This gradual change in the affinity of divalent cations after irradiation with γ -radiation, expressed by the change in ΔG° , follows the sequence of ionic size and consequently the ionic potential of these elements (Palmer & Gunter, 2001). This is because the observed change in affinity is greater for Sr²⁺ with larger size decreasing towards Mg²⁺ with smaller size. This conclusion cannot be extended to the univalent cation exchange after γ -radiation, because they display smaller changes in ΔG° for larger ions like Cs⁺. Thus, the possible changes in clinoptilolite structure after γ -radiation are not decisive for ion exchange compared to the influence of the

Table 6. Bond length (\AA) between exchange cations and oxygens in tetrahedral apices.

Bond-type	N ₀	N ₁	N ₂	N ₃	N ₄
Sr1-O2*	2.8836	2.3545	2.2800	2.3326	2.7223
Sr1-O1*	–	2.6158	2.3953	2.589	–
Sr2-O2	2.7820	–	–	–	2.8301
Sr3-O10	2.5522	2.5977	2.6137	–	2.6318
Sr3-O1*	2.1563	2.3185	2.3649	–	2.4197

*With maximum bond length 3 \AA , no bonds appeared.

ionic potential of divalent cations. In contrast, the ionic potential of univalent cations may not be important for ion exchange. Alternatively the possible structural changes affect univalent cations differently compared to divalent cations (*e.g.* greater free energy changes for the smaller ion).

Correlation between crystallographic and thermodynamic parameters

Except for amorphization, the major structural modifications observed by Rietveld refinement include shifts in extraframework positions such as Sr1 and Sr3 and occupancy changes in all exchangeable sites. It has already been mentioned that the framework structure of clinoptilolite was not refined due to sample constraints as in Part I of this study. However, being all samples part of the same original material (apart from the different doses applied to each one) and having applied the same treatment (Sr²⁺ saturation, dryness, etc.), all samples ought to exhibit identical refinement results if no structural changes introduced by radiation, which is not the case in our study. In Part I of this study major changes were reported in exchange sites present in channel A of the clinoptilolite structure (Moraetis *et al.*, 2007). In this study changes are observed also in exchange sites of channel B (exchangeable site Sr3) and this can be visualized in Fig. 10, where the site position before irradiation (N₀) and the site position after irradiation (for N₂) are exhibited. It is obvious that changes in clinoptilolite structure after irradiation affect exchangeable cations in a different manner. Without excluding the possibility of tetrahedral framework changes, we assume that if they are any changes in tetrahedrals, they are reflected on cage changes, which affect cation position. In addition, difference in bond distances between Al-O and Si-O considered risky to recognized from the present refinement. In contrast, due to the ease of cation shift (weaker attractive forces compare to attractive forces between Si-O, Al-O) difference of bond distances between extraframework cations and framework oxygens considered reliable and readily recognizable (one order of magnitude higher than Si-O, Al-O differences, see Table 6). The assumption to keep tetrahedral framework intact considered convenient approximation since the initial material N₀ fitted well with the model used (Dobelin & Armbruster, 2003). Extra verification comes from sample N₃ which exhibits partial amorphization and still Rietveld yielded satisfactory fitting (Table 4).

The increase of clinoptilolite affinity for Sr^{2+} in samples N_1 , and N_2 after irradiation with β -radiation is probably related to the increase of accessibility of more energetic sites like Sr3 which exhibits increase in occupancy. However site Sr3, which slightly shifts towards the centre of B channel (Table 6), is still a highly energetic site coordinated by 3 tetrahedral oxygens. The Sr1-O2* bond (where O2* is oxygen in tetrahedral apices after Dobelin & Armbruster, 2003) is shortened by 20 % and this can increase affinity for Sr in less energetic sites such as Sr1 and can explain the higher parts of isotherm lines ($N_{\text{Sr}} > 0.4$) for N_0 , N_1 and N_2 (Fig. 1). Moreover Sr1 site becomes coordinated also to O1* after irradiation with β -radiation (samples N_1 , N_2 , N_3) due to proximity of Sr1 to channel wall (Table 6). Sample N_3 (irradiated with the higher dose of β -radiation) shows totally different response to Sr^{2+} exchange when compared with N_1 and N_2 (Table 3). Decrease of affinity for Sr^{2+} in N_3 is in contrast with the increase of affinity for Cs^+ reported by Moraetis *et al.* (2007) for the same sample. N_3 displays a remarkable decrease of occupancy in Sr1 and Sr2 and a concomitant increase of occupancy of the more energetic site Sr3. Although the occupancy for the more energetic site Sr3 increased, the selectivity for Sr^{2+} in N_3 is lower probably because of the shift of the site towards the centre of the channel. In this case, the bond length for Sr3-O10 and Sr3-O1* is longer than 3 Å and Sr3 is not expected to be coordinated to tetrahedral apical oxygens (Table 6). The same is true also for Sr2, which shifts towards the centre of channel A (Fig. 10). Hence Sr2 and Sr3 sites are shifted towards the centre of channels A and B respectively and attracted forces become weaker since cations are drawn away from tetrahedral oxygens (Table 6), thus decreasing the affinity of N_3 for Sr^{2+} . Note that the shift of Sr1 towards the channel wall does counterbalance the shift of the more energetic Sr3 in the centre of channel B and hence the overall affinity for Sr^{2+} decreases.

Moraetis *et al.* (2007) showed structural changes after irradiation with β -radiation in less energetic sites such as Cs2 and Cs3 in channel A. In contrast Cs1 near T2 remains unaffected. In the present study Sr1 and Sr3, which are also situated near to T2 (Fig. 10), exhibit remarkable changes in the crystallographic parameters x , z . Such differences between univalent and divalent cations hosting in the irradiated samples are attributed to the synergetic effect of the ionic radii of cations hosted in the site and the probable crystal structure changes in the vicinity of the site. Moreover the larger Cs^+ with the lower ionic potential may not readily fit in a deformed structure, whereas the smaller Sr^{2+} may be fitted and attracted with stronger forces. This is supported by considering the difference of ionic radii (0.56 Å) between Cs^+ (1.69 Å) and Sr^{2+} (1.13 Å) which is comparable to the length of bond shortening (Sr1-O2*) after β -radiation (*e.g.* 0.6 Å between sample N_0 and N_2 , Table 6). Sample N_3 irradiated with β -radiation exhibits different behaviour according to the cation involved in ion exchange and this is supported both by thermodynamic parameters and crystallographic data. Thus ionic size of exchangeable cations and site specific structural deformities should be taken into consideration when assessing the ion exchange behaviour of irradiated clinoptilolite with β -radiation.

Sample N_4 exhibits a remarkable increase in affinity for Sr^{2+} . Although, this sample exhibits small changes in site coordinates, it shows a decrease in occupancy of the less energetic site Sr1 by 48 % compared to original sample (N_0). In addition, site Sr3 which shows high selectivity for Sr^{2+} exhibits increase in occupancy by 29 % and site Sr2 with the lower selectivity for Sr^{2+} exhibits increase in occupancy only by 8 %. Such cation redistribution in the different sites is expected to increase selectivity for Sr^{2+} . In sample N_3 occupancy changes were observed in site Sr3. However, in this case the decrease in selectivity for Sr^{2+} is related to the shift of the more energetic site Sr3 towards the centre of channel B as noted before. In sample N_4 , Sr3 remains near the channel wall and thus the affinity for Sr^{2+} is much higher compared to sample N_3 (Table 6). Also, Sr1 shifts slightly near the channel wall similar to sample N_3 (Table 6). It is suggested that the affinity change is due to the combined influence of occupancy change and site shifting after irradiation of zeolites either with β - or γ -radiation.

Thermogravimetric analysis in Part I of the present study showed 5 % decrease in water content in sample N_4 compared to the original sample, which is not enough to introduce major cation selectivity changes (Moraetis *et al.*, 2007). Nevertheless other changes in water molecules such as their structural positions may be critical in affinity changes especially for divalent cations, which strongly attract water molecules. However, in the present study it was not possible to examine this possibility with Rietveld refinement, given the sample physical characteristics, such as polycrystalline low purity material.

It is difficult to interpret the greater increase in affinity for Ca^{2+} in sample N_2 , since no crystal refinement was carried out for Ca^{2+} -saturated samples. The increased affinity may be related either to the increased capability of Ca^{2+} cations to diffuse in the crystal or to specific cation site structural changes. Significant decrease in water content after irradiation with β -radiation, which may enhance cation diffusion, was not observed (Moraetis *et al.*, 2007). An indication about the behaviour of Ca can be given from its similarity with Sr, since site Sr3 resembles site Ca2 in channel B (Armbruster & Gunter, 1991). It has already been mentioned that the increase in occupancy in site Sr3 is probably associated with selectivity increase, although the bond length of Sr3-O10 and Sr3-O1* slight increases (Table 6). Such changes may have influenced also Ca^{2+} exchange in site Ca2, in channel B. Finally, the hysteresis loop observed in Ca^{2+} exchange isotherm of sample N_2 may be related either to structural changes (*e.g.* clogging of Ca^{2+} in site Ca2 after β -radiation) and/or to the vicinity of site Na1 to site Ca2 (hindered Na^+ -exchange in site Na1 if Ca^{2+} is present – Armbruster, 1993), which renders the ion exchange reaction path-dependent for the specific sample.

Samples N_1 and N_2 , exhibit slight increase in affinity for Mg^{2+} and this is probably related to structural changes in cage A, since Mg^{2+} is preferably located in the centre of cage A (Armbruster, 1993; Armbruster & Gunter, 1991). The latter researchers did not report bonds of the large hydrated Mg^{2+} cation (4.28 Å according to Nightingale, 1959) with structural oxygens. Also hydrated Mg^{2+} barely fits into channel B which has dimensions 4.6×4.0 Å

(Stolz & Armbruster, 2000). The changes of thermodynamic parameters of Mg^{2+} exchange for irradiated samples are rather small compared to other divalent cations, probably due both to the large radius of hydrated Mg^{2+} and the lack of bonding with framework oxygens, which renders Mg^{2+} rather unaffected from site specific changes and structural deformities in channel A. It is interesting that the affinity for Mg^{2+} decreased after γ -radiation, in contrast to the selectivity for Ca^{2+} , which remained unchanged and the absence of major structural changes in Sr^{2+} exchangeable sites, which however display affinity increase. In conclusion, exchange of divalent cations in zeolites irradiated with γ -radiation is influenced by the ionic potential of divalent cations involved and the structural modifications in the clinoptilolite structure.

Causes of structural modifications

It has already been discussed in Part I (Moraetis *et al.*, 2007) that possible structural changes are due to formation of energetic radicals such as OH^- (Wang *et al.*, 2000), during radiolysis of water and subsequently to disruption of Al-O and Si-O bonds and final amorphization as observed in sample N₃. The absence of amorphous material in samples N₁ and N₂ is probably related to the limited amount of disrupted bonds due to production of a non-critical number of free radicals after irradiation with lower doses compared to sample N₃. However, the presence even of low number of free radicals, *e.g.* OH^- and or H^+ , may yield either cation shift (Daniels & Puri, 1986) or disruption of Al-O-Si bonds (*e.g.* by free radical) (Ermatov *et al.*, 1980; Zhang *et al.*, 1998). The aforementioned effects may cause structure bends and deformities, which successively influence hosting of extraframework cations. Structure deformities may be preferably developed in Al-bearing tetrahedra, such as the vicinity of T2. Moreover, changes observed in cation sites near T2, such as Sr1 and Sr3, are probably related with such structure deformities. Apart from the dissolution model of Moraetis *et al.* (2007), the present refinement for the Sr-saturated samples shows exchangeable site shift similar to Koyama & Takéuchi (1977), Alberti & Vezzalini (1983) and Armbruster & Gunter (1991) (black arrows in Fig. 10). Armbruster & Gunter (1991) showed a shift of cation sites Na1 and Ca2 after thermal treatment of mono-crystalline clinoptilolite towards the channel wall of cage A. Note that sites Na1 and Ca2 resemble sites Sr1 and Sr3, which also show shift parallel to a crystallographic axis.

Conclusions

Rietveld refinement and thermodynamic study of the exchange for divalent cations show further enlightening results for the influence of radiation on clinoptilolite structure. Divalent cations exhibited rather more complicated behaviour after irradiation with β -radiation compared to univalent cations. Apart from the ionic potential, which is fundamental for ion exchange of divalent cations, other

factors such as site specific structural changes influence the exchange between heterovalent cations in irradiated clinoptilolite. Ca^{2+} exchange is facilitated by β -radiation, whereas clinoptilolite shows decreased affinity for Sr^{2+} after β -radiation with the highest dose. The selectivity order obtained for the original material ($Sr > Ca > Mg$) is in accordance with the findings of other workers (*e.g.* Ames, 1961). Clinoptilolite displays almost identical selectivity for Sr^{2+} and Ca^{2+} after irradiation with β -radiation. On the other hand, after irradiation with γ -radiation clinoptilolite displays the same selectivity order as its natural counterpart. However, there are changes in equilibrium constants which indicate that although ion exchange is influenced by γ -radiation, ionic potential is still important. This may be related to structural changes in water positions, which were not refined in the present study. Mono-crystal structure refinement of irradiated clinoptilolite would probably yield interesting results for water positions and tetrahedral structure deformities.

Acknowledgements: This work was funded by the Greek Scholarship Foundation (SSF) (contract No. 34/2000-01) and by EU (INCO-Copernicus Project, Contract No. ICA-CT-2000-10019).

References

- Alietti, A. (1972): Polymorphism and crystal-chemistry of heulandites and clinoptilolites. *Am. Mineral.*, **57**, 1448-1462.
- Alberti, A. & Vezzalini, G. (1983): The thermal behaviour of heulandites: a structural study of the dehydration of Nadap heulandite. *Miner. Petrol.*, **31**, 259-270.
- Ames, L.L. (1960): The cation sieve properties of clinoptilolite. *Am. Mineral.*, **45**, 689-700.
- (1961): Cation sieve properties of the open zeolites chabazite, mordenite, erionite and clinoptilolite. *Am. Mineral.*, **46**, 1120-1131.
- (1964): Some zeolite equilibria with alkali metal cations. *Am. Mineral.*, **49**, 127-145.
- Armbruster, T. (1993): Dehydration mechanism of clinoptilolite and heulandite: Single-crystal X-ray study of Na-poor, Ca, K-, Mg-rich clinoptilolite at 100 K. *Am. Mineral.*, **78**, 260-264.
- Armbruster, T. & Gunter, M. (1991): Stepwise dehydration of heulandite-clinoptilolite from Succor Creek, Oregon, USA. A single-crystal X-ray study at 100 K. *Am. Mineral.*, **76**, 1872-1883.
- Bish, D.L. & Boak, J.M. (2001): Clinoptilolite-Heulandite Nomenclature. in "Natural zeolites: properties applications and uses", D.L. Bish & D.W. Ming, eds. *Rev. Mineral. Geochem.*, **45**, 207-216.
- Bish, D.L. & Howard, S.A. (1988): Quantitative phase analysis using the Rietveld method. *J. Appl. Crystallogr.*, **21**, 86-91.
- Bish, D.L. & Post, J.E. (1989): Rietveld refinement of crystal structures using powder X-ray diffraction data. in "Modern powder diffraction" D. L. Bish & J.E. Post, eds. *Rev. Mineral.*, **20**, 277-308.
- Boles, J.R. (1972): Composition, optical properties, cell dimensions and thermal stability of some heulandite group zeolites. *Am. Mineral.*, **57**, 1463-1493.

- Breck, D. W. (1974): Zeolite molecular sieves, structure chemistry and use. Wiley & Sons, New York, 529-570.
- Chelishchev, N.F. (1995): Use of natural zeolites at Chernobyl. in "Natural Zeolites '93: Occurrence, Properties, Us", D.W. Ming & F.A. Mumpton, eds. International Committee on Natural Zeolites, Brockport, New York, 525-532.
- Chelishchev, N.F., Berenshtein, B.G., Berenshtein, T.A., Gribanova, N.K., Martynova, N.S. (1973): Ion-exchange properties of clinoptilolites. *Dokl. Akad. Nauk*, **210**, 1110-1112.
- Cerri, G., Langella, A., Pansini, M., Cappelletti, P. (2002): Methods of determining cation exchange capacities for clinoptilolite-rich rocks of the Logudoro region in northern Sardinia, Italy. *Clays Clay Miner.*, **50**, 127-135.
- Colella, C. (1996): Ion exchange equilibria in zeolite minerals. *Miner. Depos.*, **31**, 554-562.
- Coleman, H.W. & Steele, W.G. (1999): Experimentation and Uncertainty Analysis for Engineers, 2nd edn. John Wiley & Sons, New York, 47-82.
- Coombs, D., Alberti, A., Armbruster, T., Artioli, G., Collela, C., Galli, E., Grice, J., Liebau, F., Mandarino, J., Minato, H., Nickel, E., Passaglia, E., Peacor, D., Quartieri, S., Rinaldi, R., Ross, M., Sheppard, R., Tillmanns, E., Vezzalini, G. (1998): Recommended nomenclature for zeolite minerals; report of the Subcommittee on Zeolites of the International Mineralogical Association, Commission on New Minerals and Mineral Names. *Eur. J. Mineral.*, **10**, 1037-1081.
- Daniels, E.A. & Puri, M. (1986): Physico-chemical investigations of gamma-irradiated zeolite-4A. *Radiat. Phys. Chem.* **27**, 225-227.
- Dobelin, N. & Armbruster, T. (2003): Stepwise dehydration of Sr-exchanged heulandite: A single-crystal X-ray study. *Am. Mineral.*, **88**, 527-533.
- Dyer, A., Enamy, H., Townsend, R.P. (1981): The plotting and interpretation of ion exchange isotherms in zeolites. *Sep. Sci. Technol.*, **16**, 173-183.
- Dyer, A., Chimedtsogzol, A., Campbell, L., Williams, C. (2006): Uptake of caesium and strontium radioisotopes by natural zeolites from Mongolia. *Micropor. Mesopor. Mat.*, **95**, 172-175.
- Ermatov, S.E., Mosienko, T.A., Orozbaev, R. (1980): The surface interaction and structure of an irradiated zeolite. *Russ. J. Phys. Chem.*, **54**, 1436-1438.
- Fletcher, P. & Townsend, R.P. (1981): Transition metal ion exchange in zeolites. *J. Chem. Soc., Faraday Trans.*, **1**, **77**, 497-509.
- Galav, V., Waite, T.D., Kurucz, C.N., Copper, W.J. (1997): High energy radiation destruction of polycyclic aromatic hydrocarbons in soil wash containing surfactants. *Contam. Soils*, **2**, 295-304.
- Gaines, L.G. & Thomas, H.C. (1953): Adsorption studies on clay minerals. II. Formulation of the thermodynamics of exchange adsorption. *J. Chem. Phys.*, **21**, 714-718.
- Getoff, N. & Solar, S. (1986): Radiolysis and pulse radiolysis of chlorinated phenols in aqueous solution. *Radiat. Phys. Chem.*, **28**, 443-450.
- Gottardi, G. & Galli, E. (1985): Natural Zeolites. Springer-Verlag, New York, 261-266.
- Guntelberg, E. (1926): Interaction of ions. *Z. Phys. Chem.*, **123**, 199-247.
- Hepper, E.N., Buschiazzo, D.E., Hevia G.G., Urioste, A., Antón, L. (2006): Clay mineralogy, cation exchange capacity and specific surface area of loess soils with different volcanic ash contents. *Geoderma*, **135**, 216-223.
- Hilarides, R.J., Gray, K.A., Guzzetta, J., Cortellucci, N., Sommer, C. (1994): Radiolytic degradation of 2,3,7,8-TCDD in artificially contaminated soils. *Environ. Sci. Technol.*, **28**, 2249-2258.
- Hill, R.J. & Howard, C.J. (1987): Quantitative phase analysis from neutron powder diffraction data using the rietveld method. *J. Appl. Crystallogr.*, **20**, 467-474.
- Inglezakis, V.J. (2005): The concept of "capacity" in zeolite ion-exchange systems. *J. Colloid Interface Sci.*, **281**, 68-79.
- Jama, M.A. & Yucel, H. (1990): Equilibrium studies of sodium-ammonium, potassium-ammonium and calcium-ammonium exchanges on clinoptilolite zeolite. *Sep. Sci. Technol.*, **24**, 1393-1416.
- Kielland, J. (1935): Thermodynamics of base-exchange equilibria of some different kinds of clays. *J. Soc. Chem. Ind.*, **54**, 232-234.
- Koyama, K. & Takéuchi, Y. (1977): Clinoptilolite: the distribution of potassium atoms and its role in thermal stability. *Z. Kristallogr.*, **145**, 216-239.
- Langella, A., Pansini, M., Cappelletti, P., Gennaro, B., Gennaro, M., Colella, C. (2000): NH_4^+ , Cu^{2+} , Zn^{2+} , Cd^{2+} and Pb^{2+} exchange for Na^+ in a sedimentary clinoptilolite, North Sardinia, Italy. *Micropor. Mesopor. Mat.*, **37**, 337-343.
- Loizidou, M. (1982): Ion Exchange of Lead and Cadmium with the Sodium and Ammonium forms of Some Natural Zeolites. Ph.D. Thesis, City University, London.
- McBride, M.B. (1994): Environmental Chemistry of Soils. Oxford University Press, Oxford, 73-96.
- Mercer, B.W. & Ames, L.L. (1978): Zeolite ion exchange in radioactive and municipal wastewater treatment. in "Natural Zeolites: Occurrence, Properties, Use", L.B. Sand & F.A. Mumpton, eds. Pergamon Press, Oxford, 451-461.
- Meier, W.M. & Olson, D.H. (1992): Atlas of zeolite structure types. *Zeolites*, **12**, 1-200.
- Ming, D.W. & Dixon, J.B. (1986): Clinoptilolite in South Texas. *Soil Sci. Soc. Am. J.*, **50**, 1618-1622.
- Ming, D.W. & Boettinger, J.L. (2001): Zeolites in Soil Environments: An overview. in "Natural zeolites: properties applications and uses", D.L. Bish & D.W. Ming, eds. *Rev. Mineral. Geochem.*, **45**, 323-345.
- Moraetis, D., Christidis, G., Perdikatsis, V. (2007): Ion exchange equilibrium and structural changes in clinoptilolite irradiated with β - and γ -radiation: Monovalent cations. *Am. Mineral.*, **92**, 1714-1730.
- Nightingale, E.R. (1959): Phenomenological theory of ion salvation. Effective radii of hydrated ions. *Phys. Chem.*, **63**, 1381-1387.
- Pabalan, R.T. (1994): Thermodynamics of ion exchange between clinoptilolite and aqueous solutions of Na^+/K^+ and $\text{Na}^+/\text{Ca}^{2+}$. *Geochim. Cosmochim. Acta*, **58**, 4573-4590.
- Pabalan, R.T. & Bertetti, F.P. (1994): Thermodynamics of ion exchange between $\text{Na}^+/\text{Sr}^{2+}$ solutions and the zeolite mineral clinoptilolite. *Mater. Res. Soc. Symp. Proc.*, **333**, 731-738.
- , — (1999): Experimental and modeling of ion exchange between aqueous solutions and the zeolite mineral clinoptilolite. *J. Solut. Chem.*, **28**, 367-393.

- Palmer, J.L. & Gunter, M.E. (2001): The effects of time, temperature, and concentration on Sr^{2+} exchange in clinoptilolite in aqueous solutions. *Am. Mineral.*, **86**, 431-437.
- Petrosov, I.Kh. & Jarbashian, R.T. (1999): Main Zeolite Deposits of Armenia, Armenian Academy Edition, Yerevan (in Russian).
- Petrosov, I.Kh. & Sadoyan, A.A. (1998): New Zeolite Deposits Spread in Armenia. *Proceedings of Armenian National Academy, Earth Sciences*, II, 3, 39 (in Russian).
- Robinson, S.M., Kent, T.E., Arnold, W.D. (1995): Treatment of contaminated wastewater at Oak Ridge Laboratory by zeolites and other ion exchangers. in "Natural Zeolites '93: Occurrence, Properties, Use", D.W. Ming & F.A. Mumpton, eds. International Committee on Natural Zeolites Brockport, New York, 579-586.
- Shkrob, I.A. & Trifunac, A.D. (1997): Spin-polarized H/D atoms and radiation chemistry in amorphous silica. *J. Chem. Phys.*, **107**, 2374-2385.
- Stafford, U., Kimberly, A.G., Kamat, P.V. (1994): Radiolytic and TiO_2 -assisted photocatalytic degradation of 4-dhlorophenol. A comparative study. *J. Phys. Chem.*, **98**, 6343-6351.
- Stolz, J. & Armbruster, T. (2000): Mg^{2+} , Mn^{2+} , Cd^{2+} , Sr^{2+} and Cu^{2+} exchange in heulandite single crystals: X-ray structure refinements. in "Natural Zeolites for the Third Millenium", C. Collela & F.A. Mumpton, eds. De Frede Editore, Napoli, Italy, 119-138.
- Truesdell, A.H. & Jones, B.F. (1974): WATEQ, a computer program for calculating chemical equilibria of natural waters. *J. Res. U.S. Geol. Surv.*, **2**, 233-248.
- Vaniman, D.T., Chipera, S.J., Bish, D.L., Carey, J.W., Levy, S.S. (2001): Quantification of unsaturated-zone alteration and cation exchange in zeolitized tuffs at Yucca Mountain, Nevada, USA. *Geochim. Cosmochim. Acta*, **65**, 3409-3433.
- Wang, S.X., Wang, L.M., Ewing, R.C. (2000): Electron and ion irradiation of zeolites. *J. Nucl. Mater.*, **278**, 233-241.
- Werst, D.W., Han, P., Trifunac, A.D. (1998): Radiation chemical studies in zeolites: Radical cations and zeolite catalysis. *Radiat. Phys. Chem.*, **51**, 255-262.
- Zhang, G., Xinsheng, L., Thomas, J.K. (1998): Radiation induced physical and chemical processes in zeolite materials. *Radiat. Phys. Chem.*, **51**, 135-152.

Received 16 July 2007

Modified version received 4 March 2008

Accepted 31 March 2008